Inorg. Chem. **2008**, *47*, 8912−8920

Syntheses, Characterization, and Photochromic Studies of Spirooxazine-Containing 2,2′-Bipyridine Ligands and Their Zinc(II) Thiolate Complexes

Zhihong Bao,[†,‡] Ka-Yuen Ng,[‡] Vivian Wing-Wah Yam,*[,†,‡] Chi-Chiu Ko,*[,‡,§] Nianyong Zhu,[‡] and Lixin Wu[†]

State Key Laboratory of Supramolecular Structure and Materials and College of Chemistry, Jilin University, Changchun 130012, P.R. China, Department of Chemistry, The University of Hong Kong, Pokfulam Road, Hong Kong, P.R. China, and Department of Biology and Chemistry, City University of Hong Kong, Tat Chee Avenue, Kowloon, Hong Kong, P.R. China

Received May 30, 2008

A series of photochromic spirooxazine-containing zinc(II) diimine bis-thiolate complexes were successfully synthesized, and their photophysical and photochromic properties were studied. The X-ray crystal structure of complex **1a** has also been determined. Upon excitation by UV light at 330 nm, all the ligands and complexes exhibit photochromic behavior. The thermal bleaching kinetics of the ligands and the complexes were studied in dimethylformamide at various temperatures. The photochemical quantum yields for the photochromic reactions of the ligands and complexes were also determined.

Introduction

Photochromism is defined as a reversible transformation of a chemical species having different absorption properties being induced by absorption of electromagnetic radiation.[1] In recent years, photochromic systems have been demonstrated to show potential applications in many areas such as in photochromic spectacles,[2] optical data storage,[3] molecular switches,[4] and biosensors.[5] Spiropyran/spirooxazine is one of the well-known families of photochromic molecules that undergo ring-opening reaction under ultraviolet irradiation to give the corresponding intensely colored photomerocyanine (PMC) form, which is thermally unstable and readily reverted by thermal reaction or by absorption of visible-light irradiation.[6] It has been demonstrated that the incorporation of transition metal−ligand chromophores into photochromic molecules could render a new class of photochromic coordination compounds with novel properties,[7] such as sensitized photochromism,[7a−d] electrochemical modulation,[7e,f] and fluorescence modulation.[7c,g] We previously reported the photosensitization of the spirooxazine moiety using the rhenium(I) tricarbonyl diimine complex system.[7a] We anticipated that by incorporating these versatile photochromic ligands into various metal complex systems, in

* To whom correspondence should be addressed. E-mail: wwyam@hku.hk (V.W.-W.Y.), vinccko@cityu.edu.hk (C.-C.K.). Fax: +(852)2857-1586. Tel: +(852)2859-2153.
† Jilin University.
‡ The University of Hong Kong.
§ City University of Hong Kong.

(1) Hirshberg, Y. *C. R. Acad. Sci., Paris* **1950**, *231*, 903.
(2) Christiane, S.-D.; Barbara, L.-H.; Gilles, B.; Gérard, G.; Robert, G. *J. Photochem. Photobiol. A: Chem.* **1995**, *91*, 223–232.
(3) (a) Morimoto, M.; Kobatake, S.; Irie, M. *J. Am. Chem. Soc.* **2003**, *125*, 11080–11087. (b) Yuan, W. F.; Sun, L.; Tang, H. H.; Wen, Y. Q.; Jiang, G. J.; Huang, L. J.; Song, Y. L.; Tian, H.; Zhu, D. B. *Adv. Mater.* **2005**, *17*, 156–160. (c) Xiao, S. Z.; Zou, Y.; Yu, M. X.; Yi, T.; Zhou, Y. F.; Li, F. Y.; Huang, C. H. *Chem. Commun.* **2007**, *45*, 4758–4760. (d) Corredor, C. C.; Huang, Z.-L.; Belfield, K. D.; Morales, A. R.; Bondar, M. V. *Chem. Mater.* **2007**, *19*, 5165–5173.
(4) (a) Kawata, S.; Kawata, Y. *Chem. Rev.* **2000**, *100*, 1777–1788. (b) Berkovic, G.; Krongauz, V.; Weiss, V. *Chem. Rev.* **2000**, *100*, 1741–1753. (c) Chen, C.-T.; Chou, Y.-C. *J. Am. Chem. Soc.* **2000**, *122*, 7662–7672. (d) Delden, R. A. v.; Mecca, T.; Rosini, C.; Feringa, B. L. *Chem.—Eur. J.* **2004**, *10*, 61–70.
(5) Willner, I. *Acc. Chem. Res.* **1997**, *30*, 347–356.
(6) Guglielmetti, R. In *Photochromism, Molecules and Systems*; Dürr, H., Bouas-Laurent, H., Eds.; Elsevier: Amsterdam, 1990.
(7) (a) Yam, V. W. W.; Ko, C. C.; Wu, L. X.; Wong, K. M. C.; Cheung, K. K. *Organometallics* **2000**, *19*, 1820–1822. (b) Bahr, J. L.; Kodis, G.; Garza, L.; Lin, S.; Moore, A. L.; Moore, T. A.; Gust, D. *J. Am. Chem. Soc.* **2001**, *123*, 7124–7133. (c) Yam, V. W.-W.; Ko, C.-C.; Zhu, N. *J. Am. Chem. Soc.* **2004**, *126*, 12734–12735. (d) Jukes, R. T. F.; Bozic, B.; Hartl, F.; Belser, P.; De Cola, L. *Inorg. Chem.* **2006**, *45*, 8326–8341. (e) Nagashima, S.; Murata, M.; Nishihara, H. *Angew. Chem., Int. Ed.* **2006**, *45*, 4298–4301. (f) Ngan, T.-W.; Ko, C.-C.; Zhu, N. Y.; Yam, V. W.-W. *Inorg. Chem.* **2007**, *46*, 1144–1152. (g) Ko, C.-C.; Wu, L.-X.; Wong, M.-C.; Zhu, N. Y.; Yam, V. W.-W. *Chem.—Eur. J.* **2004**, *10*, 766–776. (h) Khairutdinov, R. F.; Giertz, K.; Hurst, J. K.; Voloshina, E. N.; Voloshin, N. A.; Minkin, V. I. *J. Am. Chem. Soc.* **1998**, *120*, 12707–12708. (i) Kume, S.; Nishihara, H. *Dalton Trans.* **2008**, 3260–3271.

10.1021/ic8009755 CCC: $40.75
Published on Web 08/26/2008

particular those with rich excited-state properties, the photochromic behavior of this class of compounds could be readily tuned and perturbed without the need of tedious synthetic procedures for the organic framework. As an extension of our earlier work,[7a,g] a series of spirooxazine-containing 2,2′-bipyridine ligands and their zinc(II) bis-thiolate complexes have been synthesized. One of the complexes has been structurally characterized. Their photochromic and photophysical properties have also been studied.

Experimental Section

Materials and Reagents. *N*-Bromosuccinimide (NBS) was purchased from Sinopharm Chemical Reagent Co., Ltd. and was used as received. Thiophenol, *p*-thiocresol, *p*-chlorothiophenol, *p*-methoxythiophenol, benzene-1,2-dithiol, and 1-bromododecane were obtained from Lancaster Synthesis Limited and were used as received. Zinc acetate dihydrate was purchased from Merck Chemicals and recrystallized from water prior to use. 4,4′-Dimethyl-2,2′-bipyridine and 2,7-dihydronaphthalene were obtained from Aldrich Chemical Co. 4-Bromomethyl-4′-methyl-2,2′-bipyridine,[8] 1-nitroso-2,7-dihydroxylnaphthalene,[9] 1-dodecyl-2,3,3-trimethyl-3H-indolium iodide,[10] 1,3,3-trimethyl-9′-hydroxy-spiroindolinenaphthoxazine, and 1-dodecyl-3,3-dimethyl-9′-hydroxy-spiroindolinenaphthoxazine[11] were prepared by a slight modification of reported procedures. 4-(1,3,3-Trimethylspiroindolinenaphthoxazine-9′-oxymethyl)-4′-methyl-2,2′-bipyridine (**L1**) was synthesized according to a procedure reported by us previously.[7g] Dichloromethane (CH_2Cl_2) for physical measurements was distilled over anhydrous calcium chloride and dimethylformamide (DMF) was vacuum distilled over magnesium sulfate before use. All other reagents were of analytical grade and were used as received.

The synthetic routes for spirooxazine-containing 2,2′-bipyridine zinc(II) thiolate complexes are summarized in Scheme 1.

4-(1-Dodecyl-3,3-dimethylspiroindolinenaphthoxazine-9′-oxymethyl)-4′-methyl-2,2′-bipyridine (L2). This was prepared according to a procedure similar to that of **L1**.[7g] To a stirred suspension of 4-bromomethyl-4′-methyl-2,2′-bipyridine (100 mg, 0.38 mmol) and K_2CO_3 (110 mg, 0.8 mmol) in DMF (15 mL) was added 1.1 equiv of 1-dodecyl-3,3-dimethyl-9′-hydroxy-spiroindolinenaphthoxazine (143 mg, 0.42 mmol). The mixture was stirred at room temperature for 2 days. The resulting mixture was then poured into deionized water to precipitate the product. The crude product was then purified by column chromatography on silica gel using dichloromethane-diethyl ether (1:1 v/v) as eluent to give a pale green oil. Further purification was made by recrystallization using petroleum ether to give analytically pure **L2** as a pale blue powder. Yield: 148 mg, 0.32 mmol, 83%. ^{1}H NMR (300 MHz, $CDCl_3$, 298 K): δ 0.86 (t, J = 6.9 Hz, 3H, -$(CH_2)_{11}CH_3$), 1.21−1.23 (m, 20H, -$CH_2(CH_2)_{10}CH_3$), 1.33 (s, 6H, -$C(CH_3)_2$ on indoline), 2.44 (s, 3H, -CH_3 on bpy), 3.15−3.18 (m, 2H, -$NCH_2(CH_2)_{10}$), 5.37 (s, 2H, -OCH_2-), 6.58 (d, J = 7.7 Hz, 1H, indolinic proton at 7-position), 6.84−6.88 (m, 2H, naphthoxazinic proton at 5′-position and indolinic proton at 5-position), 7.05 (d, J = 7.2 Hz, 1H, indolinic proton at 4-position), 7.14−7.20 (m, 3H, naphthoxazinic proton at 8′-position, indolinic proton at 6-position and bipyridyl proton at 5′-position), 7.47 (d, J = 4.3 Hz, 1H, bipyridyl proton at 5-position), 7.59 (d, J = 9.0 Hz, 1H, naphthoxazinic proton at 6′-position), 7.66 (d, J = 9.0 Hz, 1H, naphthoxazinic proton at 7′-position), 7.71 (s, 1H, naphthoxazinic proton at 2′-position), 7.97 (d, J = 2.5 Hz, 2H, naphthoxazinic proton at 10′-position), 8.27 (s, 1H, bipyridyl proton at 3′-position), 8.55−8.57 (m, 2H, bipyridyl proton at 3- and 6′-positions), 8.70 (d, J = 5.0 Hz, 1H, bipyridyl proton at 6-position). Positive-ion EI mass spectrum: m/z 680 ($[M]^+$). Elemental analysis calcd (%) for $C_{45}H_{52}N_4O_2 \cdot {}^1/_2H_2O$: C 78.33, H 7.75, N 8.12. Found: C 78.22, H 7.80, N 7.99.

Scheme 1. Synthetic Routes to Spirooxazine-Containing 2,2′-Bipyridine Zinc(II) Bis-thiolate Complexes

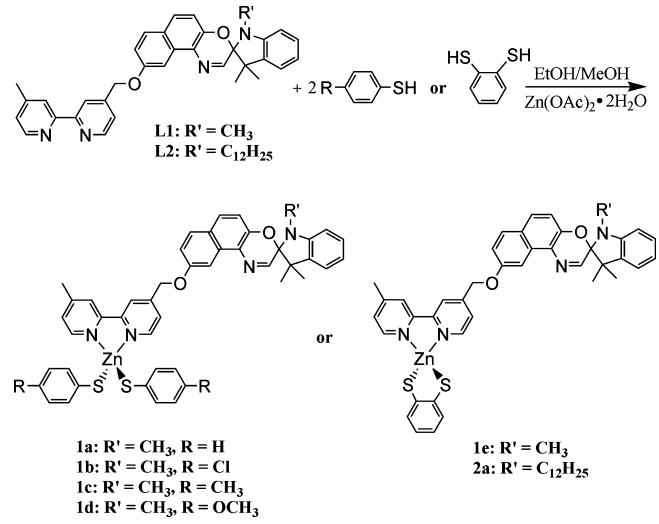

[Zn(L1)(SC_6H_5)$_2$] (1a). This was synthesized by modification of the procedures for the related zinc diimine bis(thiolate) complexes.[12] To a vigorously stirred solution of zinc acetate dihydrate (42 mg, 0.191 mmol) in ethanol (10 mL) was added benzenethiol (42 mg, 0.382 mmol). The reaction mixture was allowed to stir for 5−10 min, after which **L1** (100 mg, 0.191 mmol) was added and the resulting reaction was stirred in the dark at room temperature for 4 h. The resulting yellow precipitate was collected by suction filtration and washed with minimal amount of ethanol. Slow diffusion of diethyl ether vapor into a concentrated dichloromethane solution of the crude product afforded **1a** as greenish yellow crystals. Yield: 134 mg, 0.165 mmol, 87%. ^{1}H NMR (300 MHz, $CDCl_3$, 298 K): δ 1.35 (s, 6H, -$C(CH_3)_2$ on indoline), 2.54 (s, 3H, -CH_3 on bpy), 2.75 (s, 3H, N-CH_3 H's on indoline), 5.42 (s, 2H, -OCH_2-), 6.58 (d, J = 7.7 Hz, 1H, indolinic proton at 7-position), 6.77−6.83 (m, 6H, arenethiolate proton at 2-, 4- and 6-positions), 6.89−6.93 (m, 2H, naphthoxazinic proton at 5′-position and indolinic proton at 5-position), 7.09 (d, J = 6.7 Hz, 1H, indolinic proton at 4-position), 7.17−7.24 (m, 6H, naphthoxazinic proton at 8′-position, indolinic proton at 6-position and arenethiolate proton at 3- and 5-positions), 7.38 (d, J = 5.3 Hz, 1H, bipyridyl proton at 5′-position), 7.62−7.64 (m, 2H, naphthoxazinic proton at 6′-position and bipyridyl proton at 5-position), 7.70 (s, 1H, naphthoxazinic proton at 2′-position), 7.74 (d, J = 9.0 Hz, 1H, naphthoxazinic proton at 7′-position), 7.84 (s, 1H, bipyridyl proton at 3′-position), 7.95 (d, J = 2.5 Hz, 1H, naphthoxazinic proton at 10′-position),

(8) (a) Gould, S.; Strouse, G. F.; Meyer, T. J.; Sullivan, B. P. *Inorg. Chem.* **1991**, *30*, 2942–2949. (b) Berg, K. E.; Tran, A.; Raymond, M. K.; Abrahamsson, M.; Wolny, J.; Redon, S.; Andersson, M.; Sun, L. C.; Styring, S.; Hammarström, L.; Toftlund, H.; Akermark, B. *Eur. J. Inorg. Chem.* **2001**, *41*, 1019–1029.
(9) Marvel, C. S.; Porter, P. K. *Org. Synth.* **1941**, *1*, 411–412.
(10) Rosenzweig, H. S.; Rakhmanova, V. A.; MacDonald, R. C. *Bioconjugate Chem.* **2001**, *12*, 258–263.
(11) (a) Hosoda, M. European Patent Application EP 186364 A2, 1986. (b) Osterby, B.; McKelvey, R. D.; Hill, L. *J. Chem. Educ.* **1991**, *68*, 424–425.
(12) Yam, V. W.-W.; Pui, Y. L.; Cheung, K. K.; Zhu, N. Y. *New J. Chem.* **2002**, *26*, 536–542.

8.08 (s, 1H, bipyridyl proton at 3-position), 8.51 (d, J = 5.3 Hz, 1H, bipyridyl proton at 6′-position), 8.64 (d, J = 5.3 Hz, 1H, bipyridyl proton at 6-position). Positive-ion FAB mass spectrum: m/z 699 ([M − SC_6H_5]$^+$). Elemental analysis calcd (%) for $C_{46}H_{40}N_4O_2S_2Zn\cdot H_2O$: C 66.70, H 5.11, N 6.67. Found: C 66.34, H 5.01, N 6.93.

[Zn(L1)(SC_6H_4-*p*-Cl)$_2$](1b). This was prepared according to a procedure similar to that of **1a** except *p*-chlorobenzenethiol (55 mg, 0.382 mmol) was used in place of benzenethiol. Slow diffusion of diethyl ether vapor into a concentrated dichloromethane solution of the crude product afforded **1b** as a greenish yellow powder. Yield: 91 mg, 0.10 mmol, 54%. ^{1}H NMR (300 MHz, $CDCl_3$, 298 K): δ 1.35 (s, 6H, -C(CH_3)$_2$ on indoline), 2.57 (s, 3H, -CH_3 on bpy), 2.75 (s, 3H, N-CH_3 H's on indoline), 5.45 (s, 2H, -OCH_2-), 6.58 (d, J = 7.7 Hz, 1H, indolinic proton at 7-position), 6.77 (d, J = 8.3 Hz, 4H, arenethiolate proton at 2- and 6-positions), 6.88−6.93 (m, 2H, naphthoxazinic proton at 5′-position and indolinic proton at 5-position), 7.07−7.09 (m, 5H, indolinic proton at 4-position and arenethiolate proton at 3- and 5-positions), 7.20−7.24 (m, 2H, naphthoxazinic proton at 8′-position and indolinic proton at 6-position), 7.38 (d, J = 5.0 Hz, 1H, bipyridyl proton at 5′-position), 7.62−7.66 (m, 2H, naphthoxazinic proton at 6′-position and bipyridyl proton at 5-position), 7.72 (s, 1H, naphthoxazinic proton at 2′-position), 7.76 (d, J = 9.0 Hz, 1H, naphthoxazinic proton at 7′-position), 7.84 (s, 1H, bipyridyl proton at 3′-position), 7.97 (d, J = 2.4 Hz, 1H, naphthoxazinic proton at 10′-position), 8.15 (s, 1H, bipyridyl proton at 3-position), 8.45 (d, J = 5.0 Hz, 1H, bipyridyl proton at 6′-position), 8.61 (d, J = 5.0 Hz, 1H, bipyridyl proton at 6-position). Positive-ion FAB mass spectrum: m/z 736 ([M − SC_6H_4-Me-*p*]$^+$). Elemental analysis calcd (%) for $C_{46}H_{38}Cl_2N_4O_2S_2Zn\cdot{}^1/_2CH_2Cl_2$: C 60.77, H 4.28, N 6.10. Found: C 60.76, H 4.43, N 5.72.

[Zn(L1)(SC_6H_4-*p*-CH_3)$_2$] (1c). This was prepared according to a procedure similar to that of **1a** except *p*-methylbenzenethiol (47 mg, 0.382 mmol) was used in place of benzenethiol. Slow diffusion of diethyl ether vapor into a concentrated dichloromethane solution of the crude product afforded **1c** as yellow needle-shaped crystals. Yield: 83 mg, 0.10 mmol, 52%. ^{1}H NMR (300 MHz, $CDCl_3$, 298 K): δ 1.35 (s, 6H, -C(CH_3)$_2$ on indoline), 2.11 (s, 6H, -CH_3 on thiolate benzene), 2.55 (s, 3H, -CH_3 on bpy), 2.75 (s, 3H, N-CH_3 H's on indoline), 5.43 (s, 2H, -OCH_2-), 6.58 (d, J = 7.7 Hz, 1H, indolinic proton at 7-position), 6.63 (d, J = 7.9 Hz, 4H, arenethiolate proton at 2- and 6-positions), 6.88−6.93 (m, 2H, naphthoxazinic proton at 5′-position and indolinic proton at 5-position), 7.06−7.10 (m, 5H, indolinic proton at 4-position and arenethiolate proton at 3- and 5-positions), 7.18−7.21 (m, 2H, naphthoxazinic proton at 8′-position and indolinic proton at 6-position), 7.35 (d, J = 5.3 Hz, 1H, bipyridyl proton at 5′-position), 7.61−7.65 (m, 2H, naphthoxazinic proton at 6′-position and bipyridyl proton at 5-position), 7.72 (s, 1H, naphthoxazinic proton at 2′-position), 7.75 (d, J = 9.0 Hz, 1H, naphthoxazinic proton at 7′-position), 7.78 (s, 1H, bipyridyl proton at 3′-position), 7.96 (d, J = 2.5 Hz, 1H, naphthoxazinic proton at 10′-position), 8.10 (s, 1H, bipyridyl proton at 3-position), 8.50 (d, J = 5.3 Hz, 1H, bipyridyl proton at 6′-position), 8.64 (d, J = 5.3 Hz, 1H, bipyridyl proton at 6-position). Positive-ion FAB mass spectrum: m/z 713 ([M − SC_6H_4−Me-*p*]$^+$). Elemental analysis calcd (%) for $C_{48}H_{44}N_4O_2S_2Zn\cdot{}^1/_2H_2O$: C 68.03, H 5.35, N 6.61. Found: C 67.71, H 5.36, N 6.52.

[Zn(L1)(SC_6H_4-*p*-OCH_3)$_2$] (1d). This was prepared according to a procedure similar to that of **1a** except *p*-methoxybenzenethiol (53 mg, 0.382 mmol) was used in place of benzenethiol. Slow diffusion of diethyl ether vapor into a concentrated dichloromethane solution of the crude product afforded **1d** as yellow solid. Yield: 83 mg, 0.095 mmol, 50%. ^{1}H NMR (300 MHz, $CDCl_3$, 298 K): δ 1.37 (s, 6H, -C(CH_3)$_2$ on indoline), 2.64 (s, 3H, -CH_3 on bpy), 2.79 (s, 3H, N-CH_3 H's on indoline), 3.66 (s, 6H, -OCH_3 on thiolate benzene), 5.48 (s, 2H, -OCH_2-), 6.47 (d, J = 8.6 Hz, 4H, arenethiolate proton at 2- and 6-positions), 6.69 (d, J = 7.8 Hz, 1H, indolinic proton at 7-position), 6.87−6.92 (m, 2H, naphthoxazinic proton at 5′-position and indolinic proton at 5-position), 7.06−7.09 (m, 5H, arenethiolate proton at 3- and 5-positions, indolinic proton at 4-position), 7.18−7.24 (m, 2H, naphthoxazinic proton at 8′-position and indolinic proton at 6-position), 7.37 (d, J = 5.2 Hz, 1H, bipyridyl proton at 5′-position), 7.63−7.66 (m, 2H, naphthoxazinic proton at 6′-position and bipyridyl proton at 5-position), 7.74 (s, 1H, naphthoxazinic proton at 2′-position), 7.77 (d, J = 9.0 Hz, 1H, naphthoxazinic proton at 7′-position), 7.82 (s, 1H, bipyridyl proton at 3′-position), 7.97 (d, J = 2.5 Hz, 1H, naphthoxazinic proton at 10′-position), 8.13 (s, 1H, bipyridyl proton at 3-position), 8.54 (d, J = 5.2 Hz, 1H, bipyridyl proton at 6′-position), 8.68 (d, J = 5.2 Hz, 1H, bipyridyl proton at 6-position). Positive-ion FAB mass spectrum: m/z 729 ([M − SC_6H_4−OMe-*p*]$^+$). Elemental analysis calcd (%) for $C_{48}H_{44}N_4O_4S_2Zn\cdot CH_2Cl_2$: C 61.75, H 4.87, N 5.88. Found: C 62.01, H 4.96, N 5.68.

[Zn(L1)(SC_6H_4S-*o*)] (1e). A solution of **L1** (150 mg, 0.287 mmol) in MeOH (10 mL) was added in a dropwise manner to a solution of $Zn(OAc)_2\cdot 2H_2O$ (63 mg, 0.287 mmol) and benzene-1,2-dithiol (41 mg, 0.287 mmol) in MeOH (5 mL). The reaction mixture was stirred at room temperature for 4 h, during which yellow precipitate was formed. It was then collected by suction filtration and washed with minimal amount of methanol. Further purification could be done by slow diffusion of diethyl ether vapor into a concentrated dichloromethane solution of the crude product to give analytically pure **1e** as a yellow powder. Yield: 190 mg, 0.26 mmol, 91%. ^{1}H NMR (300 MHz, $CDCl_3$, 298 K): δ 1.35 (s, 6H, -C(CH_3)$_2$ on indoline), 2.62 (s, 3H, -CH_3 on bpy), 2.76 (s, 3H, N-CH_3 H's on indoline), 5.48 (s, 2H, -OCH_2-), 6.57 (d, J = 7.7 Hz, 1H, indolinic proton at 7-position), 6.70 (s, 2H, arenethiolate proton at 3- and 4-positions), 6.89−6.92 (m, 2H, naphthoxazinic proton at 5′-position and indolinic proton at 5-position), 7.09 (d, J = 7.7 Hz, 1H, indolinic proton at 4-position), 7.20−7.22 (m, 2H, naphthoxazinic proton at 8′-position and indolinic proton at 6-position), 7.48−7.52 (m, 3H, bipyridyl proton at 5′-position, arenethiolate proton at 2- and 5-positions), 7.63 (d, J = 2.5 Hz, 1H, bipyridyl proton at 5-position), 7.72−7.75 (m, 3H, naphthoxazinic proton at 2′, 6′, 7′-position), 7.98 (d, J = 2.5 Hz, 1H, bipyridyl proton at 3′-position), 8.09 (s, 1H, naphthoxazinic proton at 10′-position), 8.39 (s, 1H, bipyridyl proton at 3-position), 8.82 (m, 1H, bipyridyl proton at 6′-position), 8.97 (d, J = 2.5 Hz, 1H, bipyridyl proton at 6-position). Positive ion FAB mass spectrum: m/z 732 ([M]$^+$), 593 ([M−S−C_6H_4S-*o*]$^+$), 526 ([**L1**]$^+$). Elemental analysis calcd (%) for $C_{40}H_{34}N_4O_2S_2Zn\cdot CH_2Cl_2$: C 60.26, H 4.44, N 6.86. Found: C 59.91, H 4.10, N 6.94.

[Zn(L2)(SC_6H_4S-*o*)] (2a). This was prepared according to a procedure similar to that of **1e** except **L2** (195 mg, 0.287 mmol) was used in place of **L1**. Slow diffusion of diethyl ether vapor into a concentrated dichloromethane solution of the crude product afforded **2a** as a yellow solid. Yield: 224 mg, 0.253 mmol, 90%. ^{1}H NMR (300 MHz, $CDCl_3$, 298 K): δ 0.86 (t, J = 7.0 Hz, 3H, -$(CH_2)_{11}CH_3$), 1.20−1.30 (m, 20H, -$CH_2(CH_2)_{10}CH_3$), 1.32 (s, 6H, -C(CH_3)$_2$ on indoline), 2.65 (s, 3H, -CH_3 on bpy), 3.15−3.19 (m, 2H, -N$CH_2(CH_2)_{10}CH_3$), 5.42 (s, 2H, -OCH_2-), 6.58 (d, J = 7.8 Hz, 1H, indolinic proton at 7-position), 6.82 (s, 2H, arenethiolate proton at 3,4-position), 6.89−6.91 (m, 2H, naphthoxazinic proton at 5′-position and indolinic proton at 5-position), 7.07 (d, J = 6.5 Hz, 1H, indolinic proton at 4-position), 7.20−7.22 (m, 2H,

naphthoxazinic proton at 8′-position and indolinic proton at 6-position), 7.52−7.54 (m, 1H, bipyridyl proton at 5′-position), 7.61−7.64 (m, 3H, naphthoxazinic proton at 6′-position, arenethiolate proton at 2,5-position), 7.71−7.75 (m, 2H, naphthoxazinic proton at 2′-position, bipyridyl proton at 5-position), 7.79 (d, J = 4.8 Hz, 1H, naphthoxazinic proton at 7′-position), 7.99 (d, J = 2.4 Hz, 1H, bipyridyl proton at 3′-position), 8.13 (s, 1H, naphthoxazinic proton at 10′-position), 8.44 (s, 1H, bipyridyl proton at 3-position), 8.55 (d, J = 5.6 Hz, 1H, bipyridyl proton at 6′-position), 9.00 (d, J = 4.8 Hz, 1H, bipyridyl proton at 6-position). Positive ion FAB mass spectrum: m/z 885 ($[M]^+$), 746 ($[M - SC_6H_4S\text{-}o]^+$), 682 ($[\mathbf{L2}]^+$). Elemental analysis calcd (%) for $C_{51}H_{56}N_4O_2S_2Zn$: C 69.09, H 6.37, N 6.32. Found: C 69.15, H 6.11, N 6.10.

Physical Measurements and Instrumentation. ^{1}H NMR spectra were recorded on a Bruker DPX 300 (300 MHz) or a Bruker DRX 500 (500 MHz) spectrometer at 298 K. Chemical shifts (δ, ppm) were reported relative to tetramethylsilane (Me_4Si). All positive-ion fast atom bombardment (FAB) and electron impact (EI) mass spectra and electron impact (EI) were recorded on a Finnigan MAT95 mass spectrometer. Elemental analyses of the new compounds were performed on a Carlo Erba 1106 elemental analyzer by the Institute of Chemistry in Beijing or on a Flash EA 1112 elemental analyzer by the Changchun Institute of Applied Chemistry, Chinese Academy of Sciences.

Electronic absorption spectra were recorded on a Hewlett-Packard 8452A diode array spectrophotometer. Photoirradiation was carried out using a 300 W Xe (ozone-free) lamp (Oriel model 6258) and monochromatic light was obtained by passing the light through an Applied Photophysics F 3.4 monochromator.

Steady-state emission and excitation spectra at room temperature and at 77 K were recorded on a Spex Fluorolog 111 spectrofluorometer. Solid state photophysical measurements were carried out with solid samples contained in a quartz tube inside a quartz-walled Dewar flask. Measurements of the EtOH−MeOH (4:1, v/v) glass or solid state samples at 77 K were similarly conducted with liquid nitrogen filled in the optical Dewar flask. Open forms in 77 K glasses were prepared by irradiation at 365 nm at 195 K (in dry ice/acetone baths) to reach the photostationary state before immersing the samples into the liquid nitrogen bath for emission measurements.

The thermal bleaching reaction of spirooxazines is known to follow first order kinetics at various temperatures. The kinetics for the bleaching reaction were determined by measurement of the UV−vis spectral changes at various temperatures with the use of a Hewlett-Packard 8452A diode array spectrophotometer, with temperature controlled by a Lauda RM6 compact low-temperature thermostat. The first-order rate constants were obtained by taking the negative value of the slope of a linear least-squares fit of $\ln[(A - A_\infty)/(A_0 - A_\infty)]$ against time according to eq 1

$$\ln[(A - A_\infty)/(A_0 - A_\infty)] = -kt \quad (1)$$

where A, A_0, and A_∞ are the absorbance at the absorption wavelength maximum of the PMC at times t, 0, and infinity, respectively, and k is the rate constant of the reaction. The kinetic parameters were obtained by a linear least-squares fitting of $\ln(k/T)$ against $1/T$ according to the linear expression of the Eyring equation (eq 2) and $\ln k$ against $1/T$ according to the Arrhenius equation (eq 3),

$$\ln(k/T) = -(\Delta H^{\ddagger}/R)(1/T) + \ln(k_B/h) + (\Delta S^{\ddagger}/R) \quad (2)$$

$$\ln k = -E_a/RT + \ln A \quad (3)$$

where $\Delta H^{\ddagger}$ and $\Delta S^{\ddagger}$ are the changes in activation enthalpy and entropy, respectively, E_a is the activation energy, T is the temperature, and k_B, R, h, and A are the Boltzmann's constant, the universal gas constant, the Planck constant, and the frequency factor, respectively.

Chemical actinometry was employed for the photochemical quantum yield determination. Incident light intensities were taken from the average values measured just before and after each photolysis experiment using ferrioxalate actinometry.[13] In the determination of the photochemical quantum yield, the sample solutions were prepared at concentrations with absorbance slightly greater than 2.0 at the excitation wavelength. The photochemical quantum yields of the photochromic forward reaction were obtained by a linear least-squares fit of eq 4,[7g]

$$\Phi = [kV(A - A_0e^{-kt})]/[\varepsilon I(1 - e^{-kt})] \quad (4)$$

where Φ is the photochemical quantum yield, V is the volume of irradiated sample solution, I is the intensity of the light of excitation in Einsteins per second, and ε is the extinction coefficient of the PMC form, which is estimated from the averaged literature value of 4×10^4 dm^3 mol^{-1} cm^{-1}.[14,15]

Crystal Structure Determination. Crystals suitable for X-ray diffraction studies were obtained by slow diffusion of diethyl ether vapor into a dichloromethane solution of **1a**. The crystal structure was determined on a MAR diffractometer equipped with an image-plate detector.

Crystal data for **1a**: $[C_{46}H_{40}N_4O_2S_2Zn]$, formula weight = 810.31, triclinic, $P\bar{1}$ (No. 2), a = 11.832(2) Å, b = 12.058(2) Å, c = 15.333(3) Å, α = 86.26(3)°, β = 76.80(3)°, γ = 69.74(3)°, V = 1997.8(6) Å^3, Z = 2, D_c = 1.347 g cm^{-3}, μ(Mo Kα) = 0.763 mm^{-1}, $F(000)$ = 844, T = 253 K. A crystal of dimensions 0.5 × 0.3 × 0.15 mm mounted in a glass capillary was used for data collection at −20 °C on an MAR diffractometer with a 300 mm image plate detector using graphite monochromatized Mo Kα radiation (λ = 0.71073 Å). Data collection was made with a 2° oscillation step of φ, 600 s exposure time, and scanner distance at 120 mm.

One hundred images were collected and interpreted, and intensities integrated using the program DENZO.[16] The structure was solved by direct methods employing the SIR-97 program[17] on a PC. Zn, S, and many non-H atoms were located according to the direct methods and the successive least-squares Fourier cycles. Positions of other non-hydrogen atoms were found after successful refinement by full-matrix least-squares using the SHELXL-97 program[18] on a PC. The CMe_2- and NMe- groups were disordered. According to the SHELXL-97 program,[18] all 4900 independent reflections ($R_{int} = \sum|F_o^2 - F_o^2(\text{mean})|/\sum[F_o^2]$ = 0.0335, 3213 reflections larger than $4\sigma(F_o)$) from a total 8792 reflections participated in the full-matrix least-squares refinement against F^2.

(13) Murov, S. L.; Carmichael, I.; Hug, G. L. *Handbook of Photochemistry*, 2nd ed.; Marcel Dekker Inc.: New York, 1993.

(14) (a) Pozzo, J. L.; Samat, A.; Guglielmetti, R.; Keukeleire, D. D. *J. Chem. Soc., Perkin Trans.* **1993**, *2*, 1327–1332. (b) Hobley, J.; Wilkinson, F. *J. Chem. Soc., Faraday Trans.* **1996**, *92*, 1323–1330. (c) Metelitsa, A. V.; Lokshin, V.; Micheau, J. C.; Samat, A.; Guglielmetti, R.; Minkin, V. I. *Phys. Chem. Chem. Phys.* **2002**, *4*, 4340–4345.

(15) Wilkinson, F.; Hobley, J.; Naftaly, M. *J. Chem. Soc., Faraday Trans.* **1992**, *88*, 1511–1517.

(16) Otwinowski, Z.; Minor, W. *DENZO, version 1.3.0; The HKL Manual−A description of programs DENZO, XDISPLAYF, and SCALEPACK*; Gewirth, D., Ed.; Yale University: New Haven, CT, 1995;

(17) Sir97: a new tool for crystal structure determination and refinement. Altomare, A.; Burla, M. C.; Camalli, M.; Cascarano, G.; Giacovazzo, C.; Guagliardi, A.; Moliterni, A. G. G.; Polidori, G.; Spagna, R. *J. Appl. Crystallogr.* **1998**, *32*, 115.

(18) Sheldrick, G. M. *SHELX-97: Programs for Crystal Structure Analysis*, release 97−2; University of Göttingen: Göttingen, Germany, 1997.

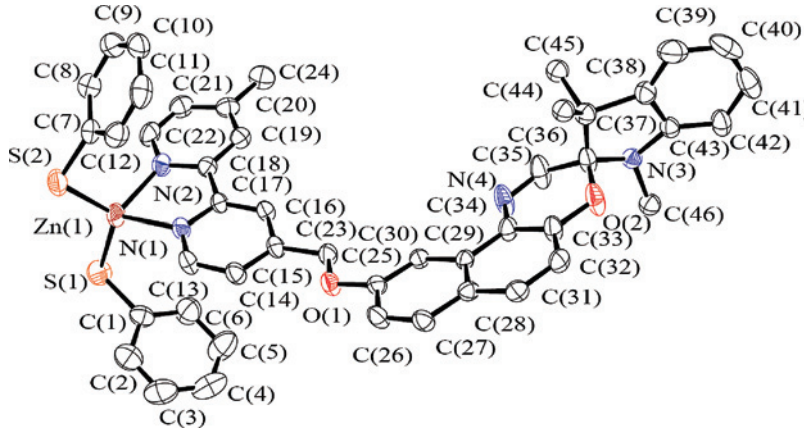

Figure 1. Perspective drawing of complex **1a** with atomic numbering. Hydrogen atoms have been omitted for clarity. Thermal ellipsoids are shown at the 30% probability level.

These reflections were in the range $-12 \le h \le 12$, $-13 \le k \le 13$, $-18 \le l \le 17$ with $2\theta_{max}$ equal to 50.66°. One crystallographic asymmetric unit consists of one formula unit. In the final stage of the least-squares refinement, all non-hydrogen atoms were refined anisotropically. H atoms were generated by the program SHELXL-97.[18] The positions of H atoms were calculated based on the riding mode with thermal parameters equal to 1.2 times that of the associated C atoms and participated in the calculation of final *R*-indices. Because the structure refinements are against F^2, *R*-indices based on F^2 are larger than (more than double) those based on *F*. For comparison with older refinements based on *F* and an OMIT threshold, a conventional index R_1 based on observed *F* values larger than $4\sigma(F_o)$ is also given (corresponding to $I \ge 2\sigma(I)$). $wR_2 = \{\sum[w(F_o^2 - F_c^2)^2]/\sum[w(F_o^2)^2]\}^{1/2}$, $R_1 = \sum||F_o| - |F_c||/\sum|F_o|$. The Goodness-of-Fit (GOF) is always based on F^2: GOF $= S = \{\sum[w(F_o^2 - F_c^2)^2]/(n - p)\}^{1/2}$, where *n* is the number of reflections and *p* is the total number of parameters refined. The weighting scheme is $w = 1/[\sigma^2(F_o^2) + (\alpha P)^2 + bP]$, where *P* is $[2F_c^2 + \mathrm{Max}(F_o^2,0)]/3$. Convergence $((\Delta/\sigma)_{max} = 0.001$, av. 0.001) for 491 variable parameters by full-matrix least-squares refinement on F^2 reaches to $R_1 = 0.0469$ and $wR_2 = 0.1153$ with a GOF of 0.941, the parameters *a* and *b* for weighting scheme are 0.067 and 0. The final difference Fourier map shows maximum rest peaks and holes of 0.478 and −0.250 e Å^{-3}, respectively.

Table 1. Crystal and Structure Determination Data for **1a**

formula	$C_{46}H_{40}N_4O_2S_2Zn$
M_r	810.31
T, [K]	253
a, [Å]	11.832(2)
b, [Å]	12.058(2)
c, [Å]	15.333(3)
α, [deg]	86.26(3)
β, [deg]	76.80(3)
γ, [deg]	69.74(3)
V, [Å^3]	1997.8(6)
crystal system	triclinic
space group	$P\bar{1}$ (No. 2)
Z	2
F(000)	844
D_c, [g cm^{-3}]	1.347
crystal dimensions, [mm]	0.5 × 0.3 × 0.15
λ, [Å (graphite monochromatized Mo Kα)]	0.71073
μ, [cm^{-1}]	7.63
collection range	$2\theta_{max} = 50.60°$ (*h*: −12 to 12; *k*: −13 to 13; *l*: −18 to 17)
oscillation, [deg]	2
no. of images collected	100
distance, [mm]	120
exposure time, [s]	600
no. of data collected	8792
no. of unique data	4900
no. of data used in refinement, [m]	3213
no. of parameters refined, [*p*]	491
R	0.0469
wR [a]	0.1153
goodness-of-fit, [*S*]	0.941
maximum shift, $(\Delta/\sigma)_{max}$	0.001
residual extrema in final difference map, [e Å^{-3}]	+0.478, −0.250

[a] $w = 1/[\sigma^2(F_o^2) + (ap)^2 + bP]$, where $P = [2F_c^2 + \mathrm{Max}(F_o^2,0)]/3$.

Results and Discussion

The substitution reactions of 4-bromomethyl-4′-methyl-2,2′-bipyridine, prepared by the bromination of 4,4′-dimethyl-2,2′-bipyridine with NBS,[8] with hydroxyl-containing spirooxazine in the presence of K_2CO_3 in DMF at room temperature gave **L1** and **L2**. Reaction of these ligands with $Zn(OAc)_2 \cdot 2H_2O$ in the presence of various substituted thiophenols in a mole ratio of 1:1:2 in ethanol or benzene-1,2-dithiol in a mole ratio of 1:1:1 in methanol afforded a series of photochromic zinc(II) bis-thiolate bipyridine complexes (Scheme 1). All of them gave satisfactory elemental analyses and were characterized by ^{1}H NMR spectroscopy and positive-ion FAB mass spectrometry. Because of the fluxional behavior associated with the thiolate ligands, broad ^{1}H NMR signals, in particular those of the arenethiolate and bipyridyl protons, were observed. Complex **1a** was also structurally characterized by X-ray crystallography.

Crystal Structure Determination. Figure 1 depicts the perspective drawing of **1a** with atomic numbering. The crystal and structure determination data and the selected bond distances and angles are summarized in Tables 1 and 2. The zinc atom adopted a distorted tetrahedral geometry. The angle subtended by the nitrogen atoms of **L1** at the zinc center, N(1)−Zn(1)−N(2), is 78.31°, which is much smaller than the ideal angle of 109° in tetrahedral geometry. The deviation from the ideal angle of 109° is due to the steric requirement of the chelating spirooxazine-containing bipyridine ligands, which is commonly observed in other related complex systems.[12,19]

The bond distance of the spiro C−O moiety, O(2)−C(36), is 1.471Å, slightly longer than the typical bond length of

Table 2. Selected Bond Lengths [Å] and Bond Angles [deg] for **1a**[a]

Zn(1)−N(1)	2.083(3)	Zn(1)−S(2)	2.2545(16)
Zn(1)−N(2)	2.096(4)	Zn(1)−S(1)	2.2596(15)
C(35)−C(36)	1.502(6)	C(36)−C(37)	1.352(13)
C(36)−N(3)	1.435(12)	O(2)−C(36)	1.471(5)
N(1)−Zn(1)−N(2)	78.31(14)	N(1)−Zn(1)−S(2)	111.84(11)
N(2)−Zn(1)−S(2)	114.31(11)	N(1)−Zn(1)−S(1)	112.09(10)
N(2)−Zn(1)−S(1)	109.86(11)	S(2)−Zn(1)−S(1)	122.16(6)
C(37)−C(36)−N(3)	105.7(8)	C(37)−C(36)−O(2)	106.7(7)
N(3)−C(36)−O(2)	109.1(6)	C(37)−C(36)−C(35)	112.7(6)
N(3)−C(36)−C(35)	112.4(6)	O(2)−C(36)−C(35)	110.0(3)

[a] Estimated standard deviations in parentheses.

C−O bond (1.43Å)[20] in other oxazine systems. This indicates the relative weakness of the bond, is also in agreement with the rationale for the photochromic reaction to involve the cleavage of this spiro carbon−oxygen bond, and is typically observed in related systems.[20]

NMR Spectroscopy. The assignments of the ^{1}H NMR signals of the ligands are based on previously reported NMR assignments of a related system.[7a,g] Slight shifts of the peaks corresponding to the bipyridyl protons are observed upon coordination to zinc, which could be explained by the perturbation of the electronic properties of bipyridine by the metal center. The chemical environments of the protons on the spirooxazine moiety are generally less affected by the coordination of zinc.

The ^{1}H NMR spectra of complexes **1a**−**1d** show broad proton signals for the bipyridine and arenethiolate protons, which is suggestive of a fluxional behavior of the system. This fluxional behavior is occurring at a rate that is comparable to the NMR time-scale and thus broad signals are observed. To provide further insight into such fluxional behavior, a variable-temperature ^{1}H NMR study on **1d** in $CDCl_3$ in the temperature range of 223−293 K was undertaken. As the temperature is decreased to 223 K the broad signals become sharper and better resolved (Figure 2, Supporting Information, Figures S1 and S2). The signal broadening is the most significant for the arenethiolate protons and the 6,6′-protons of the bipyridine, which suggested that the fluxional behavior is associated with the thiolate and bipyridine ligands.

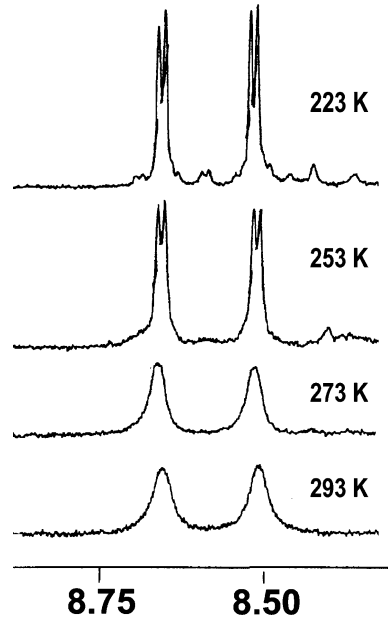

Figure 2. ^{1}H NMR signals for the 6,6′-bipyridyl protons of **1d** at various temperatures.

The proton signals for the bipyridyl protons at the 6 and 6′-positions are severely affected by the fluxional process. These signals appear in the most downfield region and do not overlap with other proton signals; therefore, a close scrutiny of the signal for the bipyridine protons at the 6 and 6′-positions gave more insight into the fluxional behavior. The variable-temperature NMR signals of the 6- and 6′-protons on bipyridine are shown in Figure 2. At 293 K, two fairly broad signals are observed at δ 8.54 and 8.68 ppm, corresponding to the proton at the 6′- and 6-positions of the bipyridine, respectively. Decreasing the temperature to 273 K results in sharper signals for these protons. As the temperature is further lowered to 253 K each signal starts to appear as a doublet. The doublet signals become more well-resolved and sharpened as the temperature reaches 223 K. Besides, a number of smaller signals could be observed near the large sharp doublets. This observation suggests that there were more than two different conformations for the complex at 223 K. The presence of the major doublets also indicates that there is a dominant form among the various conformations.

The protons at the 2- and 6-positions of the arenethiolate also display a broad signal at 6.47 ppm. This broad doublet splits and becomes two sets of doublets at 233 and 223 K (Supporting Information, Figure S1). This suggests the presence of at least two different conformations at 233 and 223 K. It is observed that the chemical environments for the arenethiolate protons in these conformations differ considerably, as reflected by the significant difference in chemical shifts of these two doublet signals. Therefore, the origin of the fluxional behavior should be closely associated with the thiolate ligands. Possible processes responsible for the observed fluxional behavior include the rapid rotation of the arenethiolate moieties about the Zn−S bond, as well as the rapid ligand scrambling brought about by the rapid dissociation−association of the arenethiolate ligand. Similar fluxional behavior has also been reported in other metal

(19) (a) Watson, A. D.; Rao, C. P.; Dorfman, J. R.; Holm, R. H. *Inorg. Chem.* **1985**, *24*, 2820–2826. (b) Highland, R. G.; Crosby, G. A. *Chem. Phys. Lett.* **1985**, *119*, 454–458. (c) Truesdell, K. A.; Crosby, G. A. *J. Am. Chem. Soc.* **1985**, *107*, 1787–1788. (d) Highland, R. G.; Brummer, J. G.; Crosby, G. A. *J. Phys. Chem.* **1986**, *90*, 1593–1598. (e) Abrahams, I. L.; Garner, C. D. *J. Chem. Soc., Dalton Trans.* **1987**, 1577–1580. (f) Jordan, K. J.; Wacholtz, W. F.; Crosby, G. A. *Inorg. Chem.* **1991**, *30*, 4588–4593. (g) Burt, J. A.; Crosby, G. A. *Chem. Phys. Lett.* **1994**, *220*, 493–496. (h) Halvorsen, K.; Crosby, G. A.; Wacholtz, W. F. *Inorg. Chim. Acta* **1995**, *228*, 81–88. (i) Anjali, K. S.; Sampanthar, J. T.; Vittal, J. J. *Inorg. Chim. Acta* **1999**, *295*, 9–17.

(20) (a) Miler-Srenger, E.; Guglielmetti, R. *Acta Crystallogr.* **1984**, *C40*, 2050. (b) Boeyens, J. C. A. *J. Cryst. Mol. Struct.* **1978**, *8*, 317–320. (c) Millini, R.; Piero, G. D.; Allegrini, P.; Crisci, L.; Malatesta, V. *Acta Crystallogr.* **1991**, *C47*, 2567. (d) Clegg, W.; Norman, N. C.; Lasch, J. G.; Kwak, W. S. *Acta Crystallogr.* **1987**, *C43*, 1222. (e) Crano, J.; Knowles, D.; Kwiatkowski, P.; Flood, T.; Ross, R.; Chiang, L.; Lasch, J.; Chadha, R.; Siuzdak, C. *Acta Crystallogr.* **1994**, *B50*, 772. (f) Chamontin, K.; Lokshin, V.; Guglielmetti, R.; Samat, A.; Pȩe, G. *Acta Crystallogr.* **1998**, *C54*, 670. (g) Allen, F. H.; Watson, O. G.; Brammer, L.; Orpen, A. G.; Taylor, R. In *International Tables for Crystallography Vol C*; Wilson, A. J. C., Ed.; Kluwer Academic: Boston, 1999; Vol. *C*, pp 685−706.

Table 3. Photophysical Data for the Ligands and the Complexes

		emission	absorption[a]
	medium (T/K)	λ_{em}/nm (τ_o/μs)	λ_{abs}/nm (ε/dm^3 mol^{-1} cm^{-1})
L1	DMF (298)	457	336 (8310), 348 (7385)
	CH_2Cl_2 (298)	*c*	280 (20880), 336 (8460), 348 sh (7470)
	glass (77)[b]	*c*	
L1(PMC)	glass (77)[b]	722 (0.20)	
L2	DMF (298)	467	336 (7990), 350 (7060)
	CH_2Cl_2 (298)	*c*	278 (22780), 336 (8890), 342 sh (8450)
	glass (77)[b]	*c*	
L2(PMC)	glass (77)[b]	724 (0.19)	
1a	DMF (298)	459	332 (11070), 348 (9735)
	CH_2Cl_2 (298)	*c*	296 (19980), 306 (18940), 332 (9680), 348 sh (7970), 380 sh (1190)
	glass (77)[b]	*c*	
1a(PMC)	glass (77)[b]	724 (0.20)	
1b	DMF (298)	459	332 (7750), 348 (6705)
	CH_2Cl_2 (298)	*c*	296 (23580), 305 (21810), 333 (9780), 341 sh (8625), 375 sh (1230)
	glass (77)[b]	*c*	
1b(PMC)	glass (77)[b]	717 (0.22)	
1c	DMF (298)	458	334 (8710), 348 (7645)
	CH_2Cl_2 (298)	*c*	296 (23260), 306 (22020), 330 (10790), 348 sh (8790), 386 sh (1090)
	glass (77)[b]	*c*	
1c(PMC)	glass (77)[b]	717 (0.19)	
1d	DMF (298)	462	330 (9335), 348 (7840)
	CH_2Cl_2 (298)	*c*	298 (22320), 306 (21110), 332 sh (9710), 348 sh (7660), 390 sh (780)
	glass (77)[b]	*c*	
1d(PMC)	glass (77)[b]	718 (0.18)	
1e	DMF (298)	468	334 (8615), 348 (6590)
	CH_2Cl_2 (298)	*c*	297 (25710), 306 (29910), 336 sh (12000), 347 sh (9025), 386 sh (710)
	glass (77)[b]	*c*	
1e(PMC)	glass (77)[b]	720 (0.20)	
2a	DMF (298)	459	330 (10050), 348 (6280)
	CH_2Cl_2 (298)	*c*	297 (28175), 307 (29750), 333 sh (14690), 344 sh (12060), 383 sh (840)
	glass (77)[b]	*c*	
2a(PMC)	glass (77)[b]	725 (0.18)	

[a] At 298 K. [b] EtOH:MeOH = 4:1 (v/v). [c] Nonemissive. PMC: photomerocyanine form.

thiolate systems.[21] The observation of a major doublet again indicated that one of the conformations is predominant.

Evidence for the fluxional process is also found in the ^{1}H NMR signals for the methyl protons of the bipyridine. At high temperature it appears as a singlet with a slightly broadened base. As the temperature is decreased another singlet emerges at the more downfield position of the peak (Supporting Information, Figure S2). The slight difference in the chemical shifts for these two signals indicated that the chemical environments for these protons are not significantly affected by the fluxional motion.

Photophysical Properties. All the complexes dissolve in DMF and CH_2Cl_2 to give clear yellow solutions. The electronic absorption spectral data of the ligands and the spirooxazine-containing complexes in CH_2Cl_2 and DMF solution at 298 K are collected in Table 3. The electronic absorption spectra of the ligands in CH_2Cl_2 at 298 K show a very intense absorption band at 280 nm, with molar extinction coefficients in the order of 10^4 dm^3 mol^{-1} cm^{-1}, which is tentatively assigned to intraligand (IL) $\pi \rightarrow \pi^*$ transitions of the bipyridine and indoline moieties. There is an additional absorption band at 336 nm with moderate intensity and molar extinction coefficient in the order of 10^3 dm^3 mol^{-1} cm^{-1}, which is assigned to the IL $\pi \rightarrow \pi^*$ transition of the naphthoxazine moiety, probably with mixing of some n $\rightarrow \pi^*$ transitions of the heterocycles. The electronic absorption spectra of complexes in CH_2Cl_2 at 298 K show very similar patterns as the free ligands at the high energy region of about 280 to 360 nm. Therefore, the absorption bands in these regions are assigned to metal-perturbed IL transitions. A red-shift of the ligand absorption band at 280 nm to about 300 nm is observed, which is probably a result of the coordination of bipyridine to zinc. The absorption of the complexes at about 330 nm is assigned to the IL $\pi \rightarrow \pi^*$ transition of the naphthoxazine moiety, and the intensity of this band is slightly increased. The most distinctive feature of the absorption spectrum of the complexes is the additional low-energy absorption shoulder at about 340 to 390 nm, which is assigned to the ligand-to-ligand charge transfer (LLCT) [π(thiolate) $\rightarrow \pi^*$(diimine)] transition, characteristic of zinc(II) diimine thiolate systems.[12,19] The dependence of the absorption wavelength of the LLCT transition on the *para* substituent of the benzenethiol is not observed in the absorption spectra. This is because the intense IL absorption of naphthoxazine at about 330 nm masked the LLCT transition band, as a consequence the LLCT band only appears as a shoulder in the spectrum. In DMF solution, this characteristic LLCT absorption cannot be readily observed. The inconspicuousness of this absorption in DMF solution is probably due to the negative solvatochromic behavior (blue-shifted as the polarity of the solvent medium increased) of this LLCT transition,[12,22] which is consequently masked by the very intense IL transitions.

Upon excitation at $\lambda = 370$ nm, all complexes in DMF solution display luminescence at about 460 nm. In view of

(21) (a) Stephen, S. O.; William, D. J. *Inorg. Chim. Acta* **2004**, *357*, 1836–1846. (b) Thérèse, A.; Pierre, T.; Marc, F.; Michel, E. *Eur. J. Inorg. Chem.* **2004**, *22*, 4502–4509.

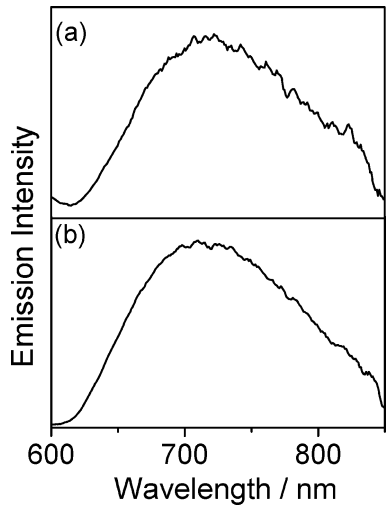

Figure 3. Emission spectra of the open form of (a) **L1** and (b) **1b** in EtOH-MeOH (4:1 v/v) glass at 77 K. Excitation wavelength at 580 nm.

Scheme 2. Photochromic Reaction of the Complexes

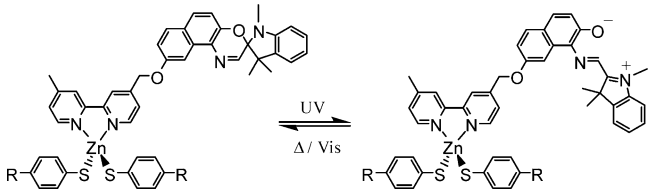

the close resemblance of these emission spectra to that of their corresponding free ligands and the insensitivity of the emission to the nature of the thiolate ligands, these emissions are tentatively assigned as fluorescence of metal-perturbed IL $\pi \rightarrow \pi^*$ origin. However, these ligands and complexes are nonemissive in CH_2Cl_2 solution, in the solid state, and in 77 K EtOH−MeOH (4:1 v/v) glass. On conversion to the open form by UV excitation, the ligands and all the zinc complexes display luminescence at about 720 nm (Figure 3) in EtOH−MeOH (4:1 v/v) glass at 77 K upon excitation into the absorption band of the PMC form at 580 nm. In view of the close resemblance of these emission maxima for the free ligands and their metal complexes, as well as the insensitivity of these emissions to the nature of the thiolate ligands, these emission bands are assigned as ligand-centered (LC) phosphorescence of the PMC form similar to those reported in the literature.[7g,23] The extended microsecond lifetime for this emission is also supportive of its triplet origin.

Photochromic Properties. On prolonged excitation at $\lambda = 330$ nm, both the ligands and the zinc complexes in DMF solution changed their color from pale yellow to blue. This is attributed to the photochromic reaction, in which the relatively weak spiro carbon−oxygen bond is photocleaved, resulting in the formation of the PMC form (Scheme 2). The much lower energy absorption of PMC at about 600 nm in the visible region is mainly due to the planarity of the two heterocyclic rings in the open form, resulting in an increase in the extended π-conjugation throughout the structure. However, these open forms are thermally unstable (half-life in the range of 7.6−9.4 s at 279 K) and quickly undergo bleaching reaction to the initial close form. These photoprocesses could be recycled for a number of times without significant decomposition as exemplified in the time dependence of absorption spectral changes at 606 nm of **1a** in DMF solution with alternating UV excitation and thermal relaxation cycles (Figure 4).

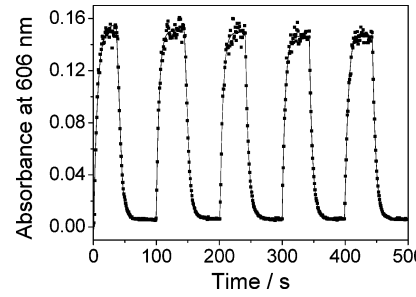

Figure 4. UV−vis absorption spectral changes of **1a** at 606 nm (■) with 326-nm excitation and the subsequent decay trace in the dark over 5 cycles. The solid lines show the theoretical nonlinear least-squares fits according to eq 4 for the excitation and eq 1 for the bleaching reaction.

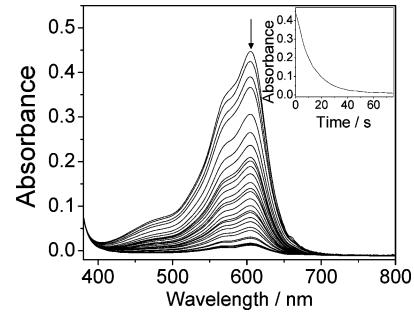

Figure 5. UV−vis absorption spectral changes of the open form of **1c** in DMF at 5.5 °C after excitation at 330 nm. The inset shows the absorption spectral trace at 608 nm with time.

Table 4. Summary of the Activation Parameters for the Bleaching Reaction of the Ligands and the Complexes in DMF Solution

	$\Delta H^{\ddagger}$/ kJ mol^{-1}	$\Delta S^{\ddagger}$/ J mol^{-1} K^{-1}	E_a/ kJ mol^{-1}
L1	73.8	−0.2	76.1
L2	72.2	−5.4	74.6
1a	75.6	5.7	78.0
1b	72.1	−6.7	77.5
1c	72.2	−6.7	74.5
1d	75.1	2.4	77.5
1e	71.2	−9.5	73.6
2a	66.6	−19.3	70.6

The kinetics for the bleaching reactions of the PMCs of the ligands and the complexes after excitation at 330 nm, were investigated in DMF solution. The thermal backward reaction results in a fading of the blue color and a decay of this absorption band (Figure 5). By monitoring the absorbance at 608 nm, the kinetics of the thermal bleaching reaction could be studied. The experiment was repeated at various temperatures to determine the activation parameters of the reaction using the Eyring and Arrhenius equations. For example, the representative UV−vis spectral changes of the open forms of complex **1c** with time, along with

(22) (a) Reichardt, C. *Angew. Chem., Int. Ed. Engl.* **1965**, *4*, 29–40. (b) Liptay, W. *Angew. Chem., Int. Ed. Engl.* **1969**, *8*, 177–188. (c) Paw, W.; Cummings, S. D.; Mansour, M. A.; Connick, W. B.; Geiger, D. K.; Eisenberg, R. *Coord. Chem. Rev.* **1998**, *171*, 125–150.
(23) Favaro, G.; Malatesta, V.; Miliani, C.; Romani, A. *J. Photochem. Photobiol. A: Chem.* **1996**, *97*, 45–52.

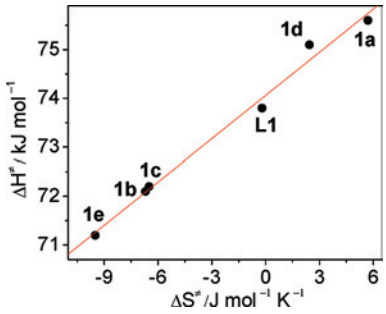

Figure 6. A plot of activation enthalpy vs activation entropy for the bleaching reaction of the open form of spirooxazine-containing ligand **L1** and its Zn(II) complexes **1a**−**1e**.

the decay curve for the absorbance at 608 nm, are shown in the inset of Figure 5. The Eyring and Arrhenius plots for the determination of the activation parameters are shown in Supporting Information, Figure S3. The thermodynamic activation parameters for the bleaching reaction of the ligands and the zinc complexes in DMF solution are collected in Table 4. The activation entropy ranges from close to zero when $\Delta H^{\ddagger}$ is large to $\Delta S^{\ddagger} = -19.3$ J mol^{-1} K^{-1} when $\Delta H^{\ddagger}$ is smaller. It has been shown that the thermodynamic parameters depend on both the nature of substituent groups on the indoline and oxazine rings, and the solvent polarities.[24] On the other hand, most of activation entropies of the ligands and complexes were found to be negative, indicating that the activated complexes are more ordered than the PMC form. An isokinetic relationship, which means a linear proportionality between $\Delta H^{\ddagger}$ and $\Delta S^{\ddagger}$, is observed. This is suggestive of a common bleaching reaction mechanism.[24] A plot of activation enthalpy versus activation entropy for the bleaching reaction of the open form of spirooxazine-containing ligand **L1** and its Zn(II) complexes is shown in Figure 6, and from the slope of the graph, the isokinetic temperature for the thermal bleaching reaction is estimated to be 295.4 ± 1.5 K.

The photochemical quantum yields of the ligands and the complexes in DMF solution at 288 K have also been estimated (Table 5). The quantum yield for the photochromic reaction of **L1** and **L2** in DMF solution at 288 K is found to be 0.60 and 0.65, respectively. The zinc complexes generally

(24) (a) Favaro, G.; Masetti, F.; Mazzucato, U.; Ottavi, G.; Allegrini, P.; Malatesta, V. *J. Chem. Soc., Faraday Trans.* **1994**, *90*, 333–338. (b) Chibisov, A. K.; Görner, H. *Phys. Chem. Chem. Phys.* **2001**, *3*, 424–431. (c) Chibisov, A. K.; Görner, H. *J. Phys. Chem. A.* **1999**, *103*, 5211–5216. (d) Metelitsa, A. V.; Micheau, J. C.; Voloshin, N. A.; Voloshina, E. N.; Minkin, V. I. *J. Phys. Chem. A.* **2001**, *105*, 8417–8422.

Table 5. Summary of the Estimated Photochemical Quantum Yields of the Photochromic Forward Reactions of the Ligands and the Complexes in DMF Solution with the Excitation at 326 nm

compound	photochemical quantum yield/Φ
L1	0.60
L2	0.65
1a	0.58
1b	0.57
1c	0.65
1d	0.54
1e	0.43
2a	0.49

possess similar quantum yields for the photochromic reaction, ranging from 0.43 to 0.65, which are in the typical range for related spirooxazine compounds.[24b,c] The quantum yields of complexes **1a**−**1d** do not appear to show a trend that correlates with the electronic properties of the thiolate ligand. This suggested that the coordination of ligands to zinc complexes has little effect on the photochromic quantum yield of the spirooxazine moiety when excited at 326 nm.

Conclusion

A series of photochromic spirooxazine-containing zinc(II) diimine bis-thiolate complexes were successfully synthesized, and their photophysical and photochromic properties were studied. Upon excitation by UV light at 330 nm, all the ligands and complexes exhibit photochromic behavior. The thermal bleaching kinetics of the ligands and the complexes were studied in DMF at various temperatures. A linear relationship between the activation enthalpy and entropy was seen, and an isokinetic temperature of 295.4 ± 1.5 K was estimated. The photochemical quantum yields for the photochromic reactions of the ligands and complexes were also determined.

Acknowledgment. We acknowledge support from Jilin University and the University of Hong Kong. This work has been supported by the National Natural Science Foundation of China and the Research Grants Council of Hong Kong Joint Research Scheme (NSFC-RGC Project No. N_HKU 737/06).

Supporting Information Available: ^{1}H NMR signals for the methyl and arenethiolate protons of **1d** at various temperatures, Eyring and Arrhenius plots for thermal bleaching reaction, and a CIF file giving crystallographic data for **1a**. This material is available free of charge via the Internet at http://pubs.acs.org.

IC8009755